Magnetic and superconducting phase diagrams of single-crystal $Er_{0.8}R_{0.2}Ni_2B_2C$ (R=Tb,Lu) and $ErNi_{1.9}Co_{0.1}B_2C$: Identification of pair-breaking mechanisms

H. Takeya
National Institute for Materials Science, 1-2-1 Sengen, Tsukuba, Ibaraki, 305-0047, Japan

M. El Massalami*
Instituto de Fisica-UFRJ, Caixa Postal 68528, 21945-970, Rio de Janeiro, Brazil
(Received 15 August 2003; published 15 January 2004)

We investigated the magnetism, superconductivity and their interplay in single crystals $Er_{0.8}R_{0.2}Ni_2B_2C$ (R=Tb,Lu) and $ErNi_{1.9}Co_{0.1}B_2C$. In contrast to Co substitution, R substitutions induce considerable modifications in the magnetism of Er sublattice: e.g., Tb (Lu) substitution enhances (reduces) T_N and critical fields. Both R substitutions introduce size effects and pinning centers; the former modifies the magnon specific heat while the latter hinders the formation of a weak ferromagnetism. The superconductivity, on the other hand, is strongly (weakly) influenced by Tb and Co (Lu) substitution. Taking $LuNi_2B_2C$ as a nonmagnetic superconducting limit, we analyzed their superconductivities, as well as that of $ErNi_2B_2C$, in terms of multiple pair breaking theory on dirty superconductors. Based on this analysis, many of their superconducting features can be explained: The breakdown of de Gennes scaling is due to the presence of multiple pair breakers, the anisotropy of $H_{c2}(T)$ is related to the magnetic anisotropy, the absence of a structure in $H_{c2}(T)$ at T_N of Lu substitution ($T_N<T_c$) is attributed to an alloying-induced destruction of phase space truncation, and the quasi parabolic temperature dependence of $H_{c2}(T)$ of Tb and Co substitutions is in part due to a saturation of antiferromagnetic correlations. For Lu substitution, the strength of magnon mediated pair breaking process(es) is substantially reduced.

DOI: 10.1103/PhysRevB.69.024509 PACS number(s): 74.70.Dd, 74.25.Dw, 74.62.Dh, 74.25.Ha

I. INTRODUCTION

The heavy members of quaternary intermetallic borocarbides RNi_2B_2C (R=Tm-Dy) manifest very interesting magnetic and superconducting phase diagrams (see, e.g., Refs. 1 and 2). These diagrams—partially driven by a nonspherical, nested Fermi surface[3,4]—reveal a (weak) interaction among the magnetic and superconducting states. The nature and strength of this interaction had been the subject of extensive investigations.[1,2] The fact that the energy of the magnetic order ($\sim k_B T_N$) is much higher than that of the superconducting condensation ($\sim k_B^2 T_c^2/E_F$) explains why the focus had been centered on tracking the influence of magnetism on superconductivity.

Eisaki *et al.*[5] reported that T_c of RNi_2B_2C scales with the corresponding de Gennes (deG) factor. Cho *et al.*,[6] on extending these investigation to $R_{1-x}R_xNi_2B_2C$, observed a deviation from this scaling even for $T_c>T_N$, such a deviation was attributed to crystalline electric field (CEF) effects. In fact, a complete breakdown of this scaling was observed for $Ho_{1-x}Dy_xNi_2B_2C$ ($x>0.2$) and interpreted in terms of a magnon-mediated pair breaking process.[6,7] Alternatively Doh *et al.*,[8] on using Ginzburg–Landau theory, suggested that the anomalous superconducting behavior of $Ho_{1-x}Dy_xNi_2B_2C$ is related to its magnetic fluctuations and order.

Upper critical field, H_{c2}, curves of RNi_2B_2C had been extensively investigated.[1,2] As an example, Bud'ko and Canfield[9] reported that $H_{c2}(T)$ of $ErNi_2B_2C$ along the easy a axis is lower than that along the hard c axis, reflecting the strong influence of the magnetic anisotropy. Moreover, a dip of $H_{c2}(T)$ at and just below T_N (much sharper along the hard axis) was observed and attributed to either a magnon-mediated process[10] or a reduction in the phase space.[11] On the other hand, Amici *et al.*[12] and Morozov[13] interpreted the nearly reentrant behavior of $H_{c2}(T)$ of $HoNi_2B_2C$ (Ref. 14) in terms of pair breaking due to nonmagnetic impurities and a reduction in electron–phonon interaction. The former pair breaking process[13,15] is possibly the predominant one in $Dy_{1-x}Lu_xNi_2B_2C$ ($x<0.2$).[6]

As evident from above there is no unified and systematic approach for identifying and evaluating pair breaking processes in these antiferromagnetic (AF) superconducting borocarbides. A particularly well suited approach is the theory of multiple pair breaking in dirty superconductors (see, e.g., Refs. 16 and 17). One of the main objectives of this work is to apply this theory for the analysis of pair breaking processes in three single crystals $Er_{0.8}Tb_{0.2}Ni_2B_2C$ ($T_c<T_N$), $Er_{0.8}Lu_{0.2}Ni_2B_2C$ ($T_c>T_N$), and $ErNi_{1.9}Co_{0.1}B_2C$ ($T_c<T_N$). These particular substituents are selected for being adequate representations of magnetic, nonmagnetic, and electronic perturbations. The identification of pair breaking processes in these compounds (as well as in the host matrix $ErNi_2B_2C$) is a useful contribution towards the elucidation of the interplay between magnetism and superconductivity in $ErNi_2B_2C$, in particular, and borocarbides in general.

It is perhaps helpful to visualize the involved electronic subsystems in these AF superconductors as being subdivided into three categories:[15] *Superconducting electrons* (predominately from Ni d band) interact very weakly with *magnetic, localized* $4f$ *electrons*. The third class is *exchange-coupling-mediating electrons*, the presence of which is independent of superconductivity. The facts that the $4f$ moments are highly

TABLE I. Superconducting critical temperatures and fields of RNi_2B_2C (R=Lu, Er), $Er_{0.8}R_{0.2}Ni_2B_2C$ (R=Lu, Tb) and $ErNi_{1.9}Co_{0.1}B_2C$. H^0_{c1} is obtained from a fit to the relation $H_{c1}(1.8\,\mathrm{K}<T<T_c)=H^0_{c1}[1-(T/T_c)^2]$. H^0_{c2} represent the zero-temperature upper critical field as obtained from multiple pair breaking analysis (see text). G is de Gennes factor.

			$H^0_{c1}\pm 10$ Oe		$H^0_{c2}\pm 0.1$ kOe	
R	G	T_c ± 0.3 K	//a	//c	//a	//c
$LuNi_2B_2C$	0	16.5[d]	~800[c]	~800[c]	88.9[d]	76[d]
$ErNi_2B_2C$	2.6	10.7[b]	~450[a]	~450[a]	14[b]	20[b]
$Er_{.8}Tb_{.2}Ni_2B_2C$	4.1	3.7	115	165	2.2	2.5
$Er_{.8}Lu_{.2}Ni_2B_2C$	2.0	10.8	585	625	14.7	23.9
$ErNi_{1.9}Co_{.1}B_2C$	2.6	3.1	45	54	0.8	1.3

[a]References 26 and 27 where virgin $M(H,2\,\mathrm{K})$ curves were used.
[b]References 9 and 28.
[c]Reference 29 where polycrystals were used.
[d]References 30 and 31.

concentrated and situated on regular lattice sites and, moreover, T_c is not very far from T_N suggest that the strength of magnetic correlations at the neighborhood of T_c is not negligible.[11] As temperature is lowered towards and below T_N, these correlations would be much increased, to the extent that a spatially periodic molecular field can be defined. The weakening of superconductivity due to this field (H_Q is its Fourier transform at wave-vector $\boldsymbol{Q}$) is usually discussed along two theoretical approaches: (i) H_Q introduces a gap in the portion of Fermi surface perpendicular to $\boldsymbol{Q}$ and as such reduces the phase space available for pairing[11] (provided that the Fermi surface is nested and the induced gap is equal to or higher than Debye temperature); (ii) H_Q induces a reduction in the electron–electron phonon-mediated coupling.[12,13,15] It is the general opinion that coexistence with AF order is permitted whenever Q^{-1} is smaller than the superconducting coherence length ξ and that strong suppression occurs whenever $Q^{-1}\gtrsim\xi$.

It is recalled that $ErNi_2B_2C$ superconducts at $T_c\simeq 11$ K and orders at $T_N\simeq 6$ K into a transverse, sinusoidally modulated spin-density wave (SDW) with $\boldsymbol{Q}_{SDW}\simeq 0.55a^*$.[18–22] A weak ferromagnetic (WF) state[23] emerges below $T_{WF}\simeq 2.2$ K, and concomitantly the SDW state is transformed into an equal-amplitude, squared-up state.[18,19]

II. EXPERIMENT

Single crystals of $Er_{0.8}Tb_{0.2}Ni_2B_2C$ (Tb substitution), $Er_{0.8}Lu_{0.2}Ni_2B_2C$ (Lu substitution), and $ErNi_{1.9}Co_{0.1}B_2C$ (Co substitution) were grown by floating zone method.[24,25] Most of the measurements were carried out on as-grown samples. Some samples were annealed at 1400 C for 100 hours (or 1050 C for overnight). We observed that annealing hardly modifies the magnetism but drastically influences the superconducting properties: On reducing lattice defects, annealing suppresses the associated pair breakers.

Physical characterization were carried out utilizing a SQUID magnetometer ($H<50$ kOe, $1.8\,\mathrm{K}<T<20$ K), a four-point transverse magnetoresistive ac bridge ($1.8\,\mathrm{K}<T<20$ K, $I\leqslant 10$ mA, $H<80$ kOe), and a zero-field semi-adiabatic calorimeter ($0.5\,\mathrm{K}<T<25$ K, precision better than 4%). For the isofield magnetization, data were collected during the warming-up cycle after field cooling (FC) or zero-field cooling (ZFC) process.

For each compound, the total specific heat C_{tot} was analyzed as a sum of an electronic C_e (C_S within the superconducting phase), a Debye C_D, a nuclear C_N, and a magnetic contribution C_M from the R sublattice. $C_N(T)$, appreciable only below 1 K, was evaluated assuming that the contribution of each nuclear spin is equal to that of its parent compound.[7] C_e and C_D were estimated based on our specific heat characterization[32] of single crystal $ErNi_2B_2C$ ($\gamma=17.5$ mJ/molK^2 and $\beta=0.206$ mJ/molK^4) which had been synthesized by the very same procedures as the ones used for this study. $C_S(T\leqslant T_c)$ was taken[33] as $3\gamma T^3/T_c^2$ which means that $C_S(T_c)-C_e(T_c)=2\gamma T_c\approx 0.14$ J/molK for Tb substitution, 0.35 J/molK for Lu substitution, and 0.11 J/molK for

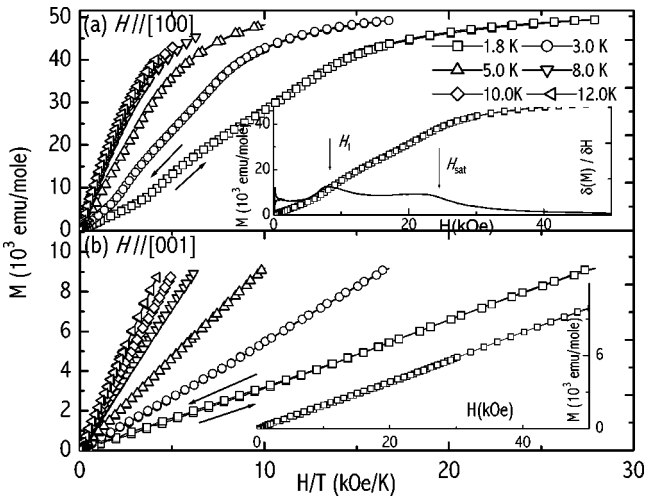

FIG. 1. Isothermal $M(H/T)$ curves of as-grown $Er_{0.8}Tb_{0.2}Ni_2B_2C$ for (a) $H\|[100]$ and (b) $H\|[001]$. The inset in each panel gives $M(H)$ at 1.8 K. In the inset of (a), the derivative at 1.8 K is also included. Similar derivative curves were used for determining (meta)magnetic critical fields.

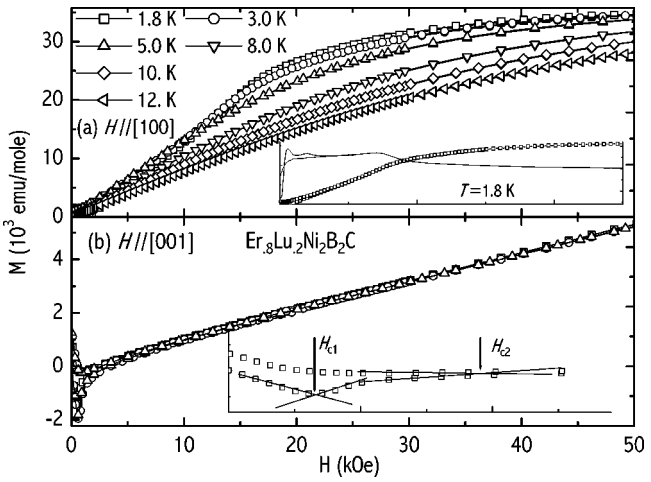

FIG. 2. Isothermal $M(H)$ curves of as grown $Er_{0.8}Lu_{0.2}Ni_2B_2C$ for (a) $H\|[100]$ and (b) $H\|[001]$. The inset in (a) shows $M(H)$ at 1.8 K together with its field derivative. The inset in (b) shows an expanded low-field isotherm (used to determine H_{c1} and H_{c2}).

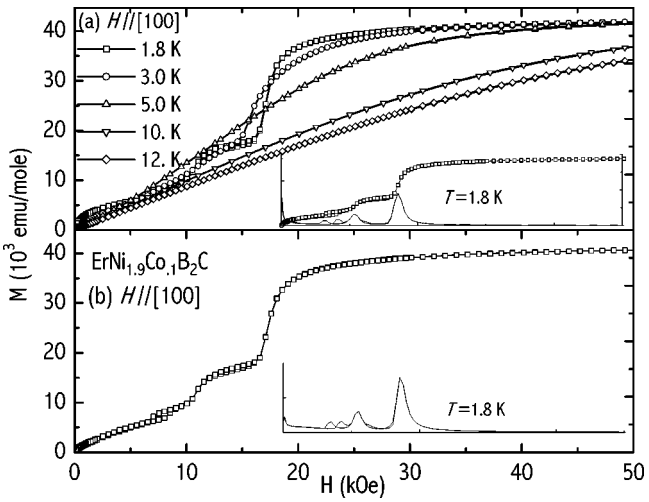

FIG. 3. (a) Isothermal $M(H\|a)$ curves of as grown $ErNi_{1.9}Co_{0.1}B_2C$. The inset shows $M(H)$ (and its field derivative) at 1.8 K. (b) $M(H\|a$ axis) curve at 1.8 K of $ErNi_{1.9}Co_{0.1}B_2C$ after being annealed at 1400 C for 100 hours.

Co substitution. For Tb and Co (Lu) substitutions, such a jump occurs in the ordered (paramagnetic) phase and amounts to ~2% (10%) of C_M which is on (greater than) the limit of our resolution. Consequently, the onset of superconductivity is resolved only in the specific heat curve of Lu substitution.

T_N was taken as the point at which $C_M(T)$ attains its maximum value while T_{WF} as the point where the slope of $C_M(T<T_N)$ breaks. H_{c1}, H_{c2}, and T_c were determined[34] from linear extrapolations of magnetoresistivity or magnetization data. Since for each sample, T_c at zero-field was determined from four different bars (two orientations for each of magnetization and resistivity), then there would be, inevitably, a weak distribution: This amounts to 0.3 K (see Table I) which is higher than the width of the superconducting transition. Further, H_{c1} was determined from only the virgin branch of low-field isothermal ZFC magnetization. $H_{c2}(T)$ curves, determined from the resistivity, agree reasonably well with those determined from the magnetization.

The de Gennes factor of the parent or Co substituted compounds is taken as $G=(g-1)^2J(J+1)$ while for $Er_{1-x}R_xNi_2B_2C$ (R=Lu,Tb) is taken as $G=xG_R+(1-x)G_{Er}$. Around T_c, the free-ion G factors are reduced by CEF effects which for the case of, say, Ho^{3+} were reported to induce an 8% reduction in G.[6] In the compound under study, the CEF effects are expect to induce an almost equal reduction in all de Gennes factors. Nevertheless, each free-ion G factor is still a convenient parameter for scaling their critical temperatures, critical fields, and the strength of both magnetic-coupling and pair-breaking processes; in fact an explicit value of a G factor is needed only for calculating the exchange scattering parameter which, in all cases, is determined from experiment (see below).

III. RESULTS AND ANALYSIS

A. Magnetization

Isothermal magnetizations of Tb substitution (Fig. 1), Lu substitution (Fig. 2), and Co substitution (Fig. 3) were measured along $H\|a$ and $H\|c$ axes. High-field $M(H)$ isotherms reveal the characteristic paramagnetic collapse for $T>T_N$ (most evident when plotted against H/T). Below T_N, $M_{001}(H)$ curves [e.g., Figs. 1(b) and 2(b)] are linear and weak, indicating that the hard character of the c axis (and the sign of the B_2^0 parameter[28]) is maintained after substitution. On the other hand, $M_{100}(H)$ isotherms [Figs. 1(a), 2(a), 3(a)] reveal a strong and nonlinear field dependence: Field-position, moments strength, and sharpness of each of the three magnetic transitions depend on the type of substitution [see inset of Figs. 1(a), 2(a), 3(a), and Table II].

TABLE II. Critical temperatures ($H=0$) and critical fields ($T=1.8$ K) of $ErNi_2B_2C$, $Er_{0.8}R_{0.2}Ni_2B_2C$ (R=Lu, Tb) and $ErNi_{1.9}Co_{0.1}B_2C$. μ_{sat} is determined at $T=1.8$ K and $H=50$ kOe (see Figs. 1–3). Values for $ErNi_2B_2C$ were taken from Refs. 23, 26, and 28.

R	T_N ±.2 K	T_{WF} ±.1 K	H_1 ±.5 kOe	H_2 ±.5 kOe	H_{sat} ±1 kOe	μ_{sat} ±.2μ_B
$ErNi_2B_2C$	5.9	2.2	7	12–14	20	8.4
$Er_{.8}Tb_{.2}Ni_2B_2C$	6.8	1	8	⋯	23	8.8
$Er_{.8}Lu_{.2}Ni_2B_2C$	4.9	1	8	11	14	7.8
$ErNi_{1.9}Co_{.1}B_2C$	5.4	2	8.5	11	17.4	7.3

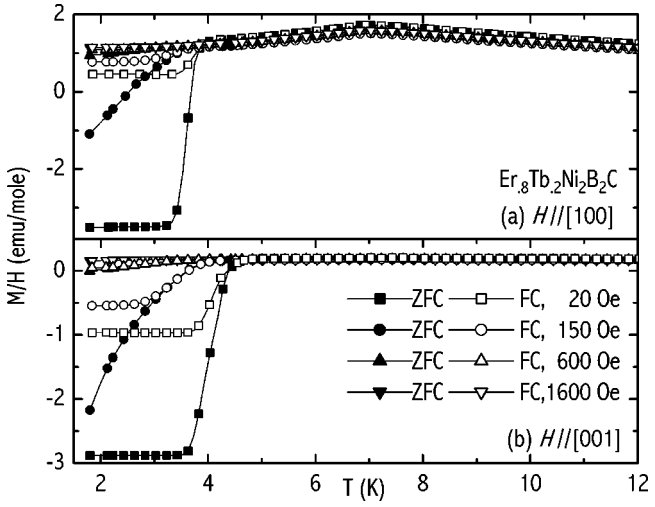

FIG. 4. T-dependent molar susceptibilities (M/H) of as-grown $Er_{0.8}Tb_{0.2}Ni_2B_2C$: (a) $H\|[100]$ while (b) $H\|[001]$. Filled (open) symbols denote a warming-up measuring branch after a ZFC (FC) process.

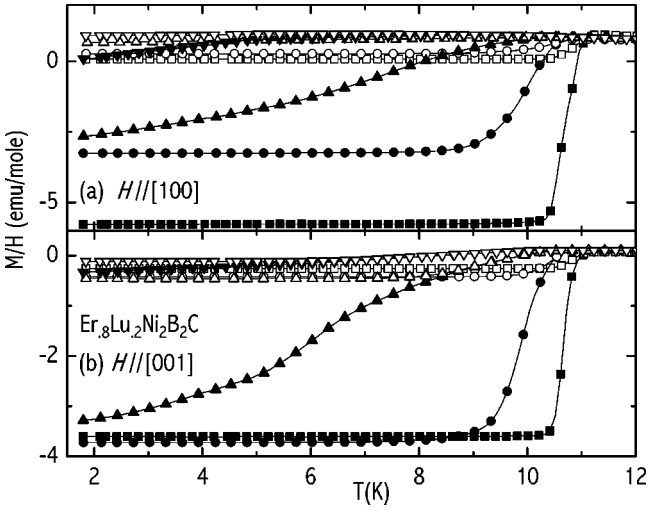

FIG. 5. T-dependent molar susceptibilities (M/H) of as-grown $Er_{0.8}Lu_{0.2}Ni_2B_2C$: (a) $H\|[100]$ while (b) $H\|[001]$. Filled (open) symbols denote a warming-up measuring branch after a ZFC (FC) process. ■, □: 20 Oe; ●, ○: 150 Oe; ▲, △: 600 Oe; ▼, ▽: 1600 Oe.

For Tb substitution [Fig. 1(a)], only two field induced transitions ($H_1 = 8$ kOe, $H_{sat} = 23$ kOe) can be unambiguously identified. Its saturated moment is $8.8\mu_B$, only 2% off the calculated weighted average. As compared to the parent compound, the *deG* factor is higher, the (meta) magnetic transitions are less sharper, the critical fields and T_N are higher, and the (average) saturated moments are stronger (see Table II). Moreover, both Er and Tb moments are coplanar[25] and possibly noncollinear (see below).

Lu substitution [Fig. 2(a)] introduces a considerable broadening of the field-induced transitions as well as a lowering of critical fields and saturation moments (see Table II). These, together with a decrease in *deG* factor and T_N, indicate a weakening of the effective magnetic couplings. Moreover, Fig. 2 suggests that the strength and anisotropy of Er^{3+} moment, being single-ion properties, are similar to those of the parent compound.

High-field $M(H)$ isotherms of Co substitution [Fig. 3(a)] reveal a relatively sharp field-induced transitions at critical fields (and with moment strength) that are very similar to those of the parent compound (see Table II): Co substitution does not modify drastically T_N, μ_{sat}, critical fields, nor the CEF single-ion character of the Er sublattice.

Isofield magnetization, measured along both *a* and *c* axes, is shown as a molar $M(T)/H$ in Figs. 4–6. The magnetic anisotropy is consistent with that observed in the isothermal magnetization. Interestingly, low-field $M(T \geqslant 1.8\,\mathrm{K})$ curves of R substitutions (Figs. 4 and 5) show no evidence of a WF-induced magnetization increase. In contrast, for Co substitution (Fig. 6), this WF-induced increase is unmistakably evident below $T_W = 2$ K; only two tenth of a degree lower than that of the parent compound.

The onset of superconductivity is evident in the magnetization curves of all substitutions and for both field orientations [Figs. 2(b), 4, 5, and 6]. As evident, an increase in H induces a reduction in T_c and a widening in the superconducting transition region.

B. Magnetoresistivity

Transverse magnetoresistivities of Tb, Lu, and Co substitutions are shown in Figs. 7–9, respectively. Evidently, $\rho_H(T_c, T_N < T < 20\,\mathrm{K})$ is almost temperature independent and tends towards 6, 4, and 15 $\mu\Omega$ cm, respectively: These values are higher than $\rho(T_c < T < 20\,\mathrm{K}) \sim 3.5\ \mu\Omega$ cm of $ErNi_2B_2C$ (Ref. 28) and $\rho(T_c < T < 20\,\mathrm{K}) \sim 1.5\ \mu\Omega$ cm of $LuNi_2B_2C$ (Ref. 35). Since the spin-disorder resistivity is 0.55–2 $\mu\Omega$ cm (just as for the parent compound), then most of the additional resistivity is due to alloying-induced disorder.

On approaching T_N, $\rho_H(T)$ of Co substitution shows a resistivity increase (see Fig. 9) which is considered as a

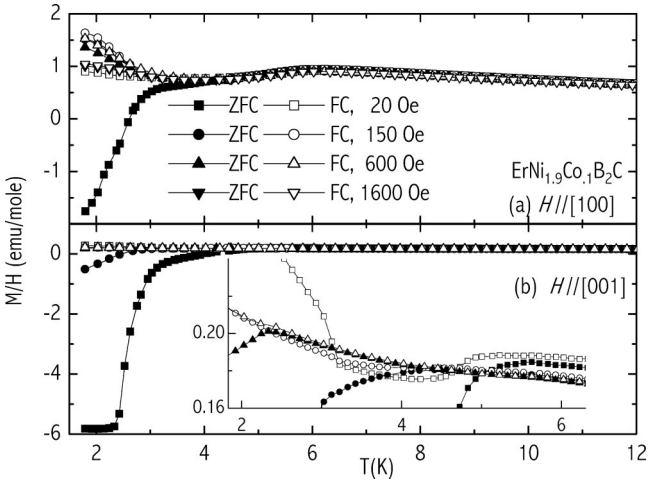

FIG. 6. T-dependent molar susceptibilities (M/H) of annealed $ErNi_{1.9}Co_{0.1}B_2C$: (a) $H\|[100]$ while (b) $H\|[001]$. The inset in (b) expands the temperature region wherein both magnetic and superconducting order are manifested. Filled (open) symbols denote a warming-up measuring branch after a ZFC (FC) process.

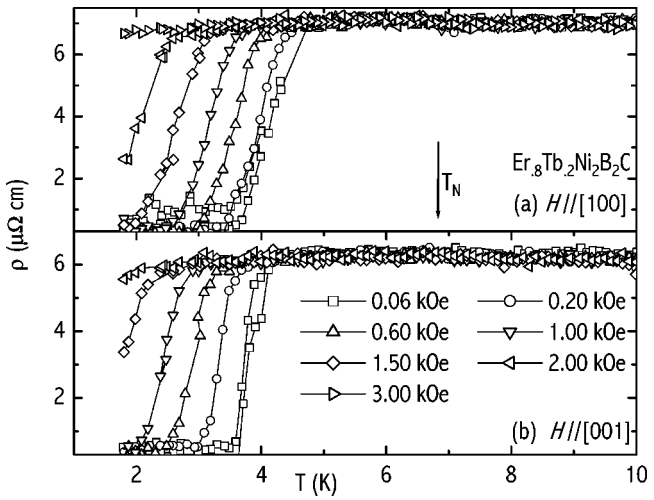

FIG. 7. Transverse magnetoresistivities of as grown $Er_{0.8}Tb_{0.2}Ni_2B_2C$ for (a) $H\|[100]$, $I\|[001]$ and (b) $H\|[001]$, $I\|[100]$.

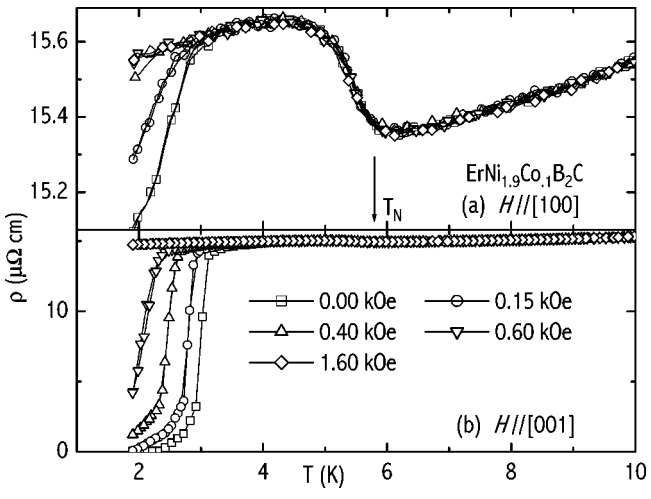

FIG. 9. Transverse magnetoresistivities of $ErNi_{1.9}Co_{0.1}B_2C$ for (a) $H\|[100]$, $I\|([001]$ and (b) $H\|[001]$, $I\|[100]$.

manifestation of partial truncation of the Fermi surface due to opening of superzone gap(s).[9] For R substitutions, such a resistivity increase is small, possibly due to an alloying-induced reduction of the superzone gapping.

The onset of superconductivity is marked by a relatively sharp drop in the resistivities (Figs. 7–9). As H is increased, the paramagnetic resistivity is hardly modified, T_c is sharply reduced, and ΔT_c is widely increased.

C. Specific heat

$C_M(T,H=0)$ of the studied substitutions (Fig. 10) manifest three distinct temperature regimes: (i) A paramagnetic phase ($T>T_N$), (ii) an intermediate regime ($T_{WF}<T<T_N$), and (iii) a low-temperature regime ($T<T_{WF}$). For R substitutions, the events at both T_N and T_{WF} are relatively broader, most probably due to alloying. Furthermore, the temperature-dependence of their $C_M(T)$ and magnetic entropies (inset of Fig. 10) are quasi similar: $C_M(T_{WF}<T<T_N)$ decreases as a power-type function, empirically found to be $0.55T^{1.6}$ for Tb substitution and $0.625T^{1.7}$ for Lu substitution. Below T_{WF}, their $C_M(T)$ are numerically comparable or even lower than their $C_N(T)$. Consequently, large uncertainties emerge, impeding a determination of a definite functional dependence. Nevertheless, it is sure that no exponential-type decay (as seen for the parent[32]) can be identified.

$C_M(T)$ of Co substitution, unlike R substitutions, is very similar to that of the parent compound: a quasi λ-type AF order at T_N and a relatively sharp change of slope at T_{WF}. In addition, two distinct thermal evolutions, separated by T_{WF}, are evident: $C_M(T_{WF}<T<T_N)$ shows a power-like dependence almost equal to that of the parent compound[32] while $C_M(T<T_{WF})$ decays with a much faster rate than that of the R substitutions but lesser than that of the parent compound.

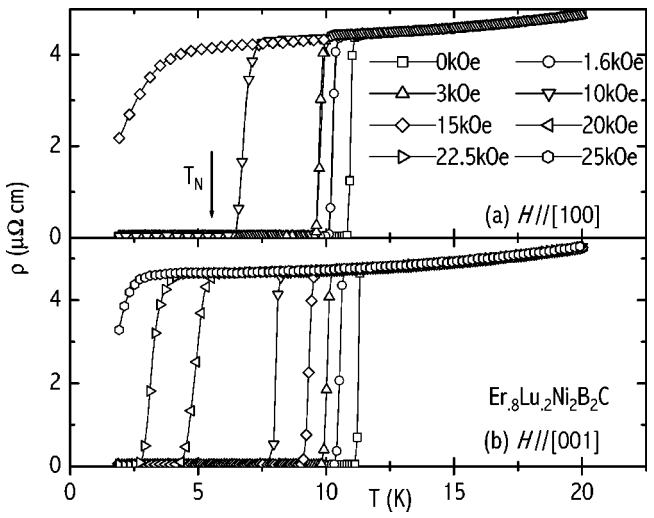

FIG. 8. Transverse magnetoresistivities of $Er_{0.8}Lu_{0.2}Ni_2B_2C$ for (a) $H\|[100]$, $I\|([001]$ and (b) $H\|[001]$, $I\|[100]$.

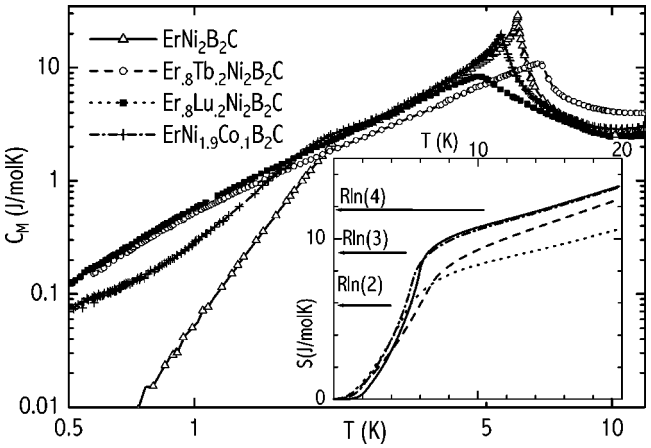

FIG. 10. Log–log plot of magnetic specific heat of $Er_{0.8}R_{0.2}Ni_2B_2C$ (R=Er, Tb, Lu) and $ErNi_{1.9}Co_{0.1}B_2C$. Evidently, except for a difference in their T_N, the overall thermal evolution of $C_M(T)$ of both $Er_{0.8}R_{0.2}Ni_2B_2C$ (R=Lu, Tb) is similar. Likewise, those of $ErNi_2B_2C$ and $ErNi_{1.9}Co_{0.1}B_2C$ are similar and moreover the temperature dependences of their magnetic entropies (see inset) are also similar. Data of $ErNi_2B_2C$ were taken from Ref. 7.

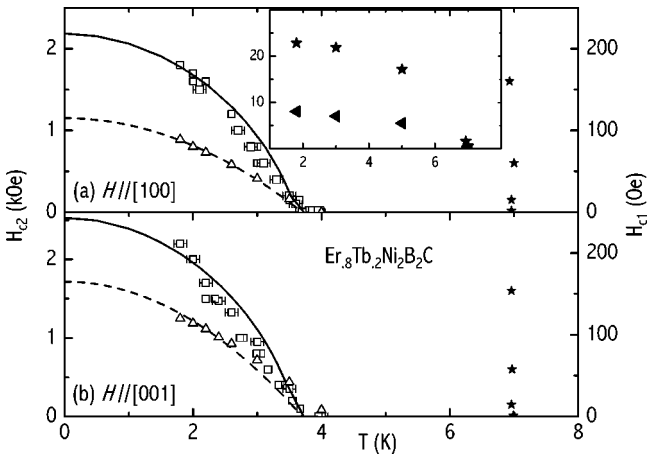

FIG. 11. Superconducting $H-T$ phase diagram of $Er_{0.8}Tb_{0.2}Ni_2B_2C$ for (a) $H\|[100]$ and (b) $H\|[001]$. ★: T_N; △: H_{c1}; □: H_{c2}. The dashed line on $H_{c1}(T)$ represents a parabolic relation (see text). The solid line represents the calculated $H_{c2}(T)$ based on multiple pair breaking theory (see text). The inset shows a partial magnetic $H-T$ phase diagram for $H\|[100]$ where ★: H_{sat} and ◀: H_2.

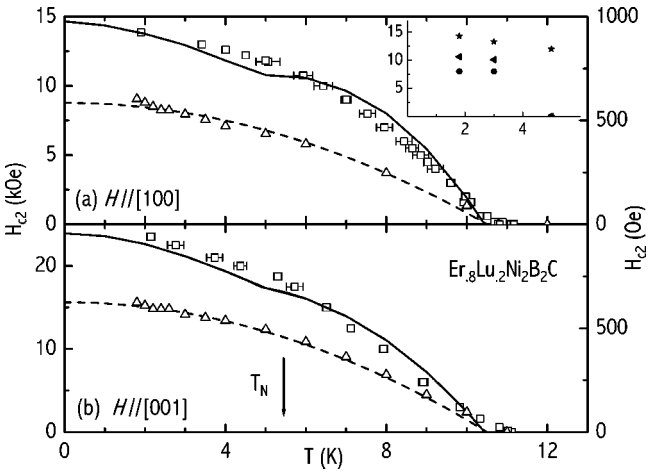

FIG. 12. Superconducting $H-T$ phase diagram of $Er_{0.8}Lu_{0.2}Ni_2B_2C$ for (a) $H\|[100]$ and (b) $H\|[001]$. ★: T_N; △: H_{c1}; □: H_{c2}. The dashed line on $H_{c1}(T)$ represents a parabolic relation (see text). The solid line represents the calculated H_{c2} curve based on multiple pair breaking theory (see text). The weak structure observed in the calculated $H_{c2}(T)$ curves is a reflection of a slight overestimation of the magnetization in the neighborhood of T_N. The inset shows a partial magnetic $H-T$ phase diagram for $H\|[100]$ where ★: H_{sat} and ◀: H_2.

Below 0.8 K, the rate of decay is reduced, the origin of which is unclear. Due to this anomaly, we were unsuccessful in carrying out a satisfactory fit of $C_M(T<T_{WF})$ using the procedures given in Refs. 7 and 32.

Thermal evolution of the magnetic entropy per one mole of chemical formulas, $S(T)$, for each substitution is shown in the inset of Fig. 10. Within the paramagnetic phase, the expected relation is well met: $S^{Er-Lu}(T)<S^{Er-Tb}(T)<S^{ErNi-Co}(T)=S^{Er}(T)$. Far below T_N, this relation is reversed: The entropy of the parent compound is the lowest while that of Lu substitution is the highest, indicating that R substitutions induce a softening of the magnon spectrum (see below).

D. Superconducting critical fields

Superconducting critical fields are shown in Figs. 11–13. Evidently, there are no reentrant features nor a spontaneous vortex state. For each substitution, the lower critical field $H_{c1}(1.8\,K<T<T_c)=H_{c1}^0[1-(T/T_c)^2]$ where H_{c1}^0 is a constant (see Table I). Such a parabolic relation was reported for polycrystalline YNi_2B_2C and $LuNi_2B_2C$.[29,36] Evidently, $H_{c1}(T)$ is weakly anisotropic and decreases along the direction $H_{c1}^{Lu}>H_{c1}^{Er-Lu}>H_{c1}^{Er}>H_{c1}^{Er-Tb}>H_{c1}^{ErNi-Co}$ (see Table I).

$H_{c2}(T)$ curves, on the other hand, show a quasi parabolic behavior (see Figs. 11–13). Moreover, $H_{c2}(\|c)>H_{c2}(\|a)$ $[\xi_{ab}<\xi_c]$, reflecting the anisotropic character of the magnetic state.[28] Such an anisotropy is opposite to the one observed in $LuNi_2B_2C$.[4,30,31] Figure 14 and Table I show that below liquid helium temperatures and along both a and c axes, $H_{c2}^{Lu}>H_{c2}^{Er-Lu}\geqslant H_{c2}^{Er}>H_{c2}^{Er-Tb}>H_{c2}^{ErNi-Co}$. Taking this inequality (as well as that of H_{c1} and T_c) as a measure of the involved pair breaking effects, it is inferred that Co substitution degrades the superconductivity much stronger than any of R substitutions. Furthermore, both Co and Tb substitutions reduce T_c to a value lower than T_N. In contrast, Lu substitution does not induce any reduction in $H_{c2}(T)$ which is very similar to that of $ErNi_2B_2C$, except that there is no structure at T_N (see Fig. 14).

Kawano-Furukawa and co-workers[27] investigated $H_{c2}(T)$ of Tb substitution down to 0.5 K using a resistivity probe: Hysteresis effects in $H_{c2}(T<1\,K)$ were observed and attributed to a field-induced realignment of the magnetization. This, acting as an additional pair breaker, induces a reduction in $H_{c2}(T)$ during the cooling branch.

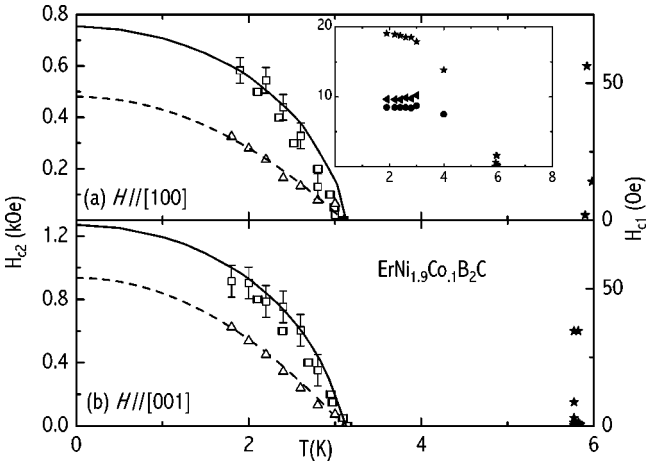

FIG. 13. Superconducting $H-T$ phase diagram of $ErNi_{1.9}Co_{0.1}B_2C$ for (a) $H\|[100]$ and (b) $H\|[001]$. ★: T_N; △: H_{c1}; □: H_{c2}. The dashed line on $H_{c1}(T)$ represents a parabolic relation (see text). The solid line represents the calculated H_{c2} curve based on multiple pair breaking theory (see text). The inset shows a partial magnetic $H-T$ phase diagram for $H\|[100]$ where ★: H_{sat} and ◀: H_2.

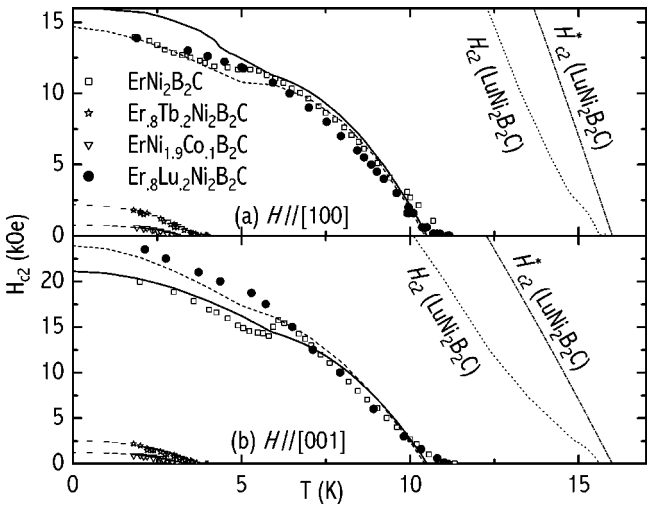

FIG. 14. A comparison of superconducting $H-T$ phase diagrams of $Er_{.8}Tb_{.2}Ni_2B_2C$, $Er_{.8}Lu_{.2}Ni_2B_2C$, and $ErNi_{1.9}Co_{0.1}B_2C$ for (a) $H\|[001]$ while (b) $H\|[100]$. The reported $H_{c2}(T)$ curves of $ErNi_2B_2C$ (Ref. 9) and $LuNi_2B_2C$ (Ref. 30) are also included. Dashed lines represent the calculation from multiple pair breaking theory (see text). Similarly, the solid lines represent such a calculation for the case of $ErNi_2B_2C$. Notice that the assumed orbital field $[H^*_{c2}(T)$, dash–dot] of $LuNi_2B_2C$ does not reproduce the observed positive curvature of $H_{c2}(T)$, presumably due to the non spherical multiband character of the Fermi surface (Refs. 30 and 31).

IV. DISCUSSION

A. Magnetic configuration

Ng and Varma[37] and Gammel *et al.*[38] interpreted the WF state in $ErNi_2B_2C$ as an ordering of *sharp* domain walls (kinks) within the equal-amplitude, squared SDW state. Recent neutron diffraction studies[18,19] revealed, on a microscopic scale, the arrangement of this WF state which (following Kawano-Furukawa *et al.*[18]) can be schematically represented along the a axis as: $..\downarrow\uparrow\uparrow\downarrow\uparrow\downarrow\uparrow\downarrow\uparrow\downarrow\uparrow\uparrow\downarrow\uparrow\downarrow\uparrow\downarrow\uparrow\downarrow\uparrow\uparrow\downarrow..$ for $z=0$ plane, while $..\downarrow\uparrow\uparrow\downarrow\uparrow\downarrow\uparrow\downarrow\uparrow\downarrow\downarrow\uparrow\downarrow\uparrow\downarrow\uparrow\downarrow\uparrow\uparrow\downarrow....$ for $z=1/2$ ($\uparrow$ and $\downarrow$ represent the Er moments). As such, the magnetic unit-cell measures $20abc$ and contains 40 Er moments. The kinks are separated by 35 Å leading to a net ferromagnetic component of magnitude $\sim 0.4\mu_B$ that coexists microscopically with superconductivity [$\xi_{ab}(2\text{ K})\approx 130$ Å].

5% Co substitution introduces no drastic modification in the overall character of this magnetic arrangement except for a change in the magnitude of the nesting vector[27] and, as a consequence, a change in the strength of the WF moment. The maintainance of the overall character of the squared-up state after Co substitution is consistent with the observed very weak variation in T_{WF} and in the magnon spectra: the latter feature explains the similarity of its $C_M(T)$ to that of the parent compound (see Fig. 10).

In contrast to Co substitution, each R substitution is expected to impart a dramatic influence on the magnetic configuration (in particular within the squared-up state) of the Er sublattice. Assuming that for $Er_{0.8}Tb_{0.2}Ni_2B_2C$ (see Sec. II A), both 4f moments maintain their original orientation[39] relative to **Q**, then a possible magnetic configuration of its equal-amplitude state is $\cdots\downarrow\uparrow\downarrow\uparrow\rightarrow\uparrow\downarrow\uparrow\downarrow\cdots\downarrow\uparrow\downarrow\uparrow\leftarrow\downarrow\uparrow\downarrow\uparrow\cdots\downarrow\uparrow\downarrow\uparrow\rightarrow\uparrow\downarrow\uparrow\downarrow\cdots$ ($\leftarrow$ and $\rightarrow$ represent Tb moments). Along similar lines, the possible magnetic configuration of the equal-amplitude state of $Er_{0.8}Lu_{0.2}Ni_2B_2C$ is $\cdots\downarrow\uparrow\downarrow\uparrow\text{-}\uparrow\downarrow\uparrow\downarrow\cdots\downarrow\uparrow\downarrow\text{-}\downarrow\uparrow\downarrow\uparrow\cdots\downarrow\uparrow\downarrow\uparrow\text{-}\uparrow\downarrow\uparrow\downarrow\cdots$ (a dash represents a nonmagnetic site). Such a random distribution of R impurities introduces two additional effects: A segmentation of the above-mentioned Er sublattice arrangement and a perturbation of the modulated states. The segmentation imposes different boundary conditions on the magnon propagation and as such modifies the magnon spectra away from the continuous-type spectra of the parent compound.[7] Then, in agreement with Fig. 10, $C_M(T)$ of such doped compounds must be different from that of the parent compound. Judging from their low-temperature $C_M(T)$ and entropy, it is inferred that R substitution induces a softening in their magnon spectra. Further, assuming that the size distributions of the segments (due to each R substituent) are similar, then their $C_M(T)$ should be similar as well: Indeed this is the case at lower temperatures (see Fig. 10).

Random distribution of R substituents, by its very nature, constitutes a strong perturbation on the modulated magnetic states. Within the squared-up, equal-amplitude state, the kinks separation would be drastically modified: In the parent compound there is one kink for every 10 chemical unit cells while after R substitution, there is, on average, one R impurity for every five chemical unit-cells. For minimizing their energy, the kinks would then preferentially reside on a substituent-site. As such, a formation of weak ferromagnetism would be highly suppressed: indeed no (or highly reduced[40]) WF state is evident in their magnetization curves. Then, the observed change of slope in the specific heats (see Fig. 10) is just a manifestation of an onset and/or complete development of the equal-amplitude squared-up state at T_{WF} (maintaining the conventional nomenclature): WF state is highly reduced (possibly quenched altogether) on R substitution but survives Co substitution.

B. Pair breaking mechanisms

The complete replacement of Lu by Er in $LuNi_2B_2C$ introduces additional effects such as exchange scattering, electromagnetic, spin polarization, phase space truncation, magnon induced electron–electron repulsion, or magnon induced reduction of electron-phonon coupling.[10–13,15–17] To identify which set of interactions are operating in $ErNi_2B_2C$ and in the doped compounds, we confronted the experimental $H_{c2}(T)$ curves of Figs. 11–14 with the prediction of the theory of multiple pair breaking of dirty superconductors (satisfying the condition mentioned in Ref. 17). The calculations are based on the following expression:[17]

$$\ln(T_{c0}/T)=a_+\Psi\left(\frac{1}{2}+\rho_+\right)+a_-\Psi\left(\frac{1}{2}+\rho_-\right)-\Psi\left(\frac{1}{2}\right),$$

$$a_\pm=\frac{1}{2}\pm(\lambda_{so}-\lambda_m)/4\gamma,$$

TABLE III. λ_m, α, and λ_{so} of the studied compounds. λ_m was calculated from the zero-field T_c while α and λ_{so} were obtained from a fit of $H_{c2}(T)$ to the theory (see text). It was assumed that $M(T,H_{c2}) \approx M(T,H_{fix})$, where H_{fix} is as given in this table. The anisotropic isofield $M(T,15\,\text{kOe})$ of $ErNi_2B_2C$ were taken from Fig. 6 of Ref. 28.

			H_{fix}(kOe)		$\alpha(\pm 0.05)$		$\lambda_{so}(\pm 0.1)$	
R	G	λ_m	//a	//c	//a	//c	//a	//c
$ErNi_2B_2C$	2.55	0.130	15	15	0.1	0.1	0.4	0.6
$Er_{.8}Tb_{.2}Ni_2B_2C$	4.1	0.255	1.6	1.6	0.6	0.6	2.0	2.5
$Er_{.8}Lu_{.2}Ni_2B_2C$	2.0	0.132	10	10	0.16	0.1	1.4	1.2
$ErNi_{1.9}Co_{.1}B_2C$	2.55	0.261	1.6	1.6	0.7	0.4	0.3	0.3

$$\rho_{\pm} = \frac{T_{c0}}{2T}\left[0.281\frac{H_{c2}+4\pi M}{H^*_{c2}(0)} + \frac{1}{2}(\lambda_{so}+\lambda_m) \pm i\gamma\right],$$

$$\gamma = \left\{\left(0.281\alpha\frac{H_{c2}+4\pi M+H_{ef}}{H^*_{c2}(0)}\right)^2 - \frac{1}{4}(\lambda_{so}-\lambda_m)^2\right\}^{1/2},$$

where Ψ is the digamma function and

(i) λ_m is the exchange scattering parameter given by $cN(E_F)I_{ex}G/2k_BT_{c0}$ where $c=1/6$, $N(E_F)=4.8$ states/eV cell is the density of states at the Fermi level,[41] I_{ex} is the exchange interaction (for $ErNi_2B_2C$, it is estimated to be 308 K), and G is the de Gennes factor. In these magnetically concentrated superconductors, λ_m was calculated from the corresponding zero-field T_c: As such it is not strictly the temperature–independent pair breaking parameter that appears in the Abrikosov–Gorkov theory. Rather it represents a sum of all zero-field pair breakers;

(ii) $H^*_{c2}(0\,\text{K})=76$ kOe is the orbital field while $T_{c0}(0\,\text{Oe})=16$ K is the critical temperature, both derived from $LuNi_2B_2C$;[30,31]

(iii) $M(T,H_{c2})$ is the volume magnetization which, for convenience, was assumed to be approximately equal to $M(T,H_{fix})$ where H_{fix} is given in Table III. The concentration of the magnetic ions $N \simeq 1.5\,10^{22}\,\text{cm}^{-3}$ was calculated from the parameters of $ErNi_2B_2C$;

(iv) $H_{ef}(T)$ is the effective exchange field taken as $H_{ef}(T)=H_{ef}(0\,\text{K})B_J(gJ\mu_BH_{c2}/k_BT)$, where $H_{ef}(0\,\text{K})=cI_{ex}(g_J-1)J/\mu_B$ and $B_J(x)$ is the Brillouin function.[42] In this analysis, $H_{ef}(0\,\text{K}) \simeq 1150$ kOe;

(v) α is the Maki parameter; and

(vi) λ_{so} is the spin–orbit scattering parameter.

In our analysis, the only free parameters are α and λ_{so}: all other parameters are fixed by experimental conditions. The calculated $H_{c2}(T)$ curves are shown in Figs. 11–14 while the fit parameters α and λ_{so} are given in Table III. We observed that the values of α and λ_{so} are not totally independent: This should be expected since, in the limit of strong spin–orbit scattering, only their ratio α/λ_{so} influences $H_{c2}(T)$.[17] Moreover, physical reasoning has to be invoked for narrowing their fitting range. As such, and considering the approximations used, the obtained values of α and λ_{so} should be judged only on qualitative grounds. Nevertheless, it is assuring to note that in all cases the thermal evolution as well as the anisotropy of $H_{c2}(T)$ are in reasonable agreement with experiments. For $ErNi_2B_2C$, the fit is very good for temperatures away from T_N reflecting the well-known limitation of the above equation in accounting for the magnon-mediated and the phase space truncation processes. However, as mentioned above, each of these processes is drastically weakened by R substitutions: For $H_{c2}(T)$ of $Er_{0.8}Lu_{0.2}Ni_2B_2C$, this explains the absence of a dip at T_N. Interestingly, the latter feature and the quasi-parabolic character of $H_{c2}(T)$ can be taken as an indication that the magnon mediated pair breaking processes are not dominant in these doped samples.

For both Tb and Co substitutions, a strong λ_m (see Table III) induces a strong reduction in T_c to the extent that $T_c < T_N$. Moreover, for the range $T<T_c<T_N$, the quasi magnetic saturation suggests that the evolution of $H_{c2}(T)$ should be quasi-parabolic: This is indeed the case (see Figs. 11 and 13).

The evolution of λ_m across the studied compounds (see Table III) does not scale with the deG factor: This confirms the earlier report of breakdown of de Gennes scaling in borocarbides.[6] It is worth empathizing that the cause of this breakdown varies according to the situation. For Co substitution, λ_m includes both electronic and magnetic perturbations: As compared to $LuNi_2B_2C$ (16 K), T_c of $LuNi_{1.9}Co_{0.1}B_2C$ (12 K) (Refs. 35 and 43) is depressed due to electronic perturbations. On the other hand, T_c of $ErNi_2B_2C$ (11 K) and of $ErNi_{1.9}Co_{0.1}B_2C$ (3 K) are determined from the action of both perturbations. Similarly λ_m of $Er_{0.8}Tb_{0.2}Ni_2B_2C$ (Refs. 44–46) is not purely an Abrikosov–Gorkov-type, otherwise T_c (using $I_{ex}=308$ K) should be 7 K. The fact that this calculated T_c is in the neighborhood of T_N suggests that the critical fluctuation is a possible additional pair breaker that reduces T_c to 4 K. Finally, Lu substitution should induce a decrease in λ_m; however, its T_c is only slightly increased. A similar weak increase in T_c was reported for $Ho_{0.8}Lu_{0.2}Ni_2B_2C$ (8.5 K)[47] and $Er_{0.8}Y_{0.2}Ni_2B_2C$ (11 K).[48] As a comparison, T_c of $Lu_{0.8}Y_{0.2}Ni_2B_2C$ is 15 K.[49] It is highly possible that for $Er_{0.8}Lu_{0.2}Ni_2B_2C$, the expected increase in T_c is offset by a decrease caused by a combination of lattice defects and appreciable AF correlations.

The evolution of α and λ_{so} across the studied compounds

is given in Table III. α, which is considered negligible for $LuNi_2B_2C$ case,[50] is increased for $ErNi_2B_2C$ and for the alloyed compounds. λ_{so}, on the other hand, does not show a systematic evolution, not even for different orientations of the same compound, possibly due to its sensitivity to impurity/defect contents.

V. CONCLUSION

Three different types of substitutions in $ErNi_2B_2C$ were carried out so as to elucidate the influence of substitution on its magnetism, superconductivity and their interplay. 5% Co substitution hardly modifies T_{WF}, T_N, H_1, H_2, and H_{sat}. In contrast, the magnetism of $ErNi_2B_2C$ is noticeably modified on 20% *R* substitution: Tb substitution, on the one hand, enhances deG factor and magnetic correlations, leading to an increase in T_N and in the critical fields. Lu substitution, on the other hand, decreases deG factor and weakens the magnetic bonds, leading to a decrease in T_N and H_{sat}. Each of *R* substitutions, unlike Co substitution, introduces two additional effects: (i) Magnetic segmentation (size effects) leading to a modification in the magnon spectrum, and (ii) pinning centers that accommodate the magnetic kinks. As a consequence, the former modifies the thermal evolution of the magnetic specific heat while the latter hinders the formation of the WF state.

Superconductivity of each compound is considered as being derived from the nonmagnetic superconducting $LuNi_2B_2C$ after an introduction of multiple pair breaking processes. Accordingly, their superconductivities were analyzed in terms of multiple pair breaking theory of dirty superconductors. In this analysis all parameters, except α and λ_{so}, were fixed. The agreement between calculated and measured $H_{c2}(T)$ curves is satisfactory. Based on this analysis, the following superconducting features are well explained: The strong reduction in T_c of both Tb and Co substitutions is due to the large increase in λ_m, the breakdown of de Gennes scaling is related to a failure of λ_m to scale with the deG factor, the anisotropy of $H_{c2}(T)$ is related to the anisotropy of the magnetic state, the absence of a structure in $H_{c2}(T)$ at T_N of Lu substitution is associated with the influence of alloying on phase space truncation, and the quasi parabolic temperature dependence of $H_{c2}(T)$ of Tb and Co substitutions is associated with the saturation of AF correlations. For Lu substitution, alloying induces a reduction in the effectiveness of magnon mediated pair breaking processes.

Improvements of our analysis to include a better approximation of $H_{ef}(T)$, $M(T,H_{c2})$, and $\lambda_m(T)$ in particular below T_N (as well as the extension of this analysis to other borocarbides) are in progress.

ACKNOWLEDGMENTS

We are grateful to Dr. H. Kawano-Furukawa for critical reading and communication of their results on $Er_{0.8}Tb_{0.2}Ni_2B_2C$ and $ErNi_{1.9}Co_{0.1}B_2C$ prior to publication. We are also grateful to Dr. F. A. Chaves, Dr. R. E. Rapp, and R. E. M. Briones for specific heat measurements.

*Electronic mail: massalam@if.ufrj.br

[1] P. C. Canfield, P. L. Gammel, and D. J. Bishop, Phys. Today **51**, 40 (1998).
[2] K.-H. Müller and V. N. Narozhnyi, Rep. Prog. Phys. **94**, 943 (2001).
[3] J. Y. Rhee, X. Wang, and B. N. Harmon, Phys. Rev. B **51**, 15 585 (1995).
[4] S. B. Dugdale, M. A. Alam, I. Wilkinson, R. J. Hughes, I. R. Fisher, P. C. Canfield, T. Jarlborg, and G. Santi, Phys. Rev. Lett. **83**, 4824 (1999).
[5] H. Eisaki, H. Takagi, R. Cava, B. Batlogg, J. J. Krajewski, W. F. Peck, Jr., K. Mizuhashi, J. Lee, and S. Uchida, Phys. Rev. B **50**, 647 (1994).
[6] B. K. Cho, P. C. Canfield, and D. C. Johnston, Phys. Rev. Lett. **77**, 163 (1996).
[7] M. El Massalami, R. E. Rapp, F. A. Chaves, H. Takeya, and C. Chaves, Phys. Rev. B **67**, 224407 (2003).
[8] H. Doh, M. Sigrist, B. K. Cho, and S.-I. Lee, Phys. Rev. Lett. **83**, 5350 (1999).
[9] S. L. Bud'ko and P. C. Canfield, Phys. Rev. B **61**, R14 932 (2000).
[10] T. V. Ramakrishnan and C. M. Varma, Phys. Rev. B **24**, 137 (1981).
[11] K. Machida, C. M. Nokura, and T. Matsubara, Phys. Rev. B **22**, 2307 (1980).
[12] A. Amici, P. Thalmeier, and P. Fulde, Phys. Rev. Lett. **84**, 1800 (2000).
[13] A. I. Morozov, JETP Lett. **63**, 734 (1996).
[14] K. Krug, M. Heinecke, and K. Winzer, Physica C **267**, 321 (1996).
[15] K. Levin, M. J. Nass, C. Ro, and G. S. Grest, in *Superconductivity in Magnetic and Exotic Materials*, edited by T. Matsubara and A. Kotani (Springer-Verlag, Berlin, 1984), Springer Series in Solid-State Sciences 52, p. 104.
[16] R. D. Parks, in *Superconductivity*, edited by P. R. Wallace (Gordon and Breach, 1969), p. 625.
[17] O. Fisher, in *Magnetic Superconductors*, edited by K. H. J. Buschow and E. P. Wohlfarth (Elsevier Science Publishers B. V., 1990), Chap. 6, p. 465.
[18] H. Kawano-Furukawa, H. Takeshita, M. Ochiai, T. Nagata, H. Yoshizawa, N. Furukawa, H. Takeya, and K. Kadowaki, Phys. Rev. B **65**, 180508 (2002).
[19] S.-M. Choi, J. W. Lynn, D. Lopez, P. L. Gammel, P. C. Canfield, and S. L. Bud'ko, Phys. Rev. Lett. **87**, 107001 (2001).
[20] J. Zarestky, C. Stassis, A. I. Goldman, P. C. Canfield, P. Dervenagas, B. K. Cho, and D. C. Johnston, Phys. Rev. B **51**, 678 (1995).
[21] S. K. Sinha, J. W. Lynn, T. E. Grigereit, Z. Hossain, L. C. Gupta, R. Nagarajan, and C. Godart, Phys. Rev. B **51**, 681 (1995).
[22] J. W. Lynn, S. Skanthakumar, Q. Huang, S. K. Sinha, Z. Hossain, L. Gupta, R. Nagarajan, and C. Godart, Phys. Rev. B **55**, 6584 (1997).
[23] P. C. Canfield, S. L. Bud'ko, and B. K. Cho, Physica C **262**, 249 (1996).
[24] H. Takeya, T. Hirano, and K. Kadowaki, Physica C **256**, 220 (1996).

[25] H. Takeya, E. Habuta, H. Kawano-Furukawa, T. Ooba, and K. Hirata, J. Magn. Magn. Mater. **226**, 269 (2001).
[26] H. Kawano, H. Takeya, H. Yoshizawa, and K. Kadowki, J. Phys. Chem. Solids **60**, 1053 (1999).
[27] H. Kawano-Furukawa, private communication.
[28] B. K. Cho, P. C. Canfield, L. L. Miller, D. C. Johnston, W. P. Beyermann, and A. Yatskar, Phys. Rev. B **52**, 3684 (1995).
[29] H. Takagi, R. J. Cava, H. Eisaki, J. O. Lee, K. Mizuhashi, B. Batlogg, S. Uchida, J. J. Krajewski, and W. F. Pech, Physica C **228**, 389 (1994).
[30] V. Metlushko, U. Welp, A. Koshelev, I. Aranson, G. W. Crabtree, and P. C. Canfield, Phys. Rev. Lett. **79**, 1738 (1997).
[31] S. V. Shulga, S. L. Drechsler, G. Fuchs, K. H. Muller, K. Winzer, M. Heinecke, and K. Krug, Phys. Rev. Lett. **80**, 1730 (1998).
[32] M. El Massalami, R. E. Rapp, E. F. Chagas, H. Takeya, J. Flores, and C. M. Chaves, J. Phys. Soc. Jpn. **71**, 582 (2002).
[33] M. El Massalami, R. E. Rapp, and H. Takeya, in *Studies in High Temperature Superconductors*, edited by A. Narlikar (Nova Science, New York, 2003), Vol. 45.
[34] Although determination of T_c, H_{c1}, and H_{c2} is a matter of controversy, a choice of a specific criterion (Refs. 9, 28, 29, 36, and 51) would not alter our conclusions significantly.
[35] K. O. Cheon, I. R. Fisher, V. G. Kogan, P. C. Canfield, P. Miranovic, and P. L. Gammel, Phys. Rev. B **58**, 6463 (1998).
[36] K. Ghosh, S. Ramakrishnan, A. Grover, and G. Chandra, Phys. Rev. B **52**, 68 (1995).
[37] T. K. Ng and C. M. Varma, Phys. Rev. Lett. **78**, 330 (1997).
[38] P. L. Gammel, B. Barber, D. Lopez, A. P. Ramirez, D. J. Bishop, S. L. Bud'ko, and P. C. Canfield, Phys. Rev. Lett. **84**, 2497 (2000).
[39] Similar moment orientations were suggested for the cases of $Y_{0.6}Tb_{0.4}Ni_2B_2C$ (Ref. 52) and $Er_{0.5}Tb_{0.5}Ni_2B_2C$ (Ref. 53).
[40] Indeed, the WF state in $Tb_{0.8}Y_{0.2}Ni_2B_2C$ is much reduced in comparison with that of $TbNi_2B_2C$ (Ref. 54).
[41] L. F. Matthias, Phys. Rev. B **49**, 13 279 (1994).
[42] S. E. Lambert, J. W. Chen, and M. B. Maple, Phys. Rev. B **30**, 6379 (1984).
[43] H. Schmidt and H. F. Braun, Phys. Rev. B **55**, 8497 (1997).
[44] Z. Q. Peng, K. Krug, and K. Winzer, Physica C **317–318**, 441 (1999).
[45] A. Rustom, A. D. Hillier, and R. J. Cywinski, J. Magn. Magn. Mater. **177–188**, 1153 (1998).
[46] A. D. Hillier, R. Cywinski, and C. Ritter, Physica B **276–278**, 658 (2000).
[47] J. Freudenberger, G. Fuchs, K. Nenkov, A. Handstein, M. Wolf, A. Kreyssig, K.-H. Muller, M. Lowenhaupt, and L. Schultz, J. Magn. Magn. Mater. **187**, 309 (1998).
[48] M. D. Lan, T. J. Chang, and C. S. Liaw, J. Phys. Chem. Solids **59**, 1285 (1998).
[49] J. Freudenberger, S. L. Drechsler, G. Fuchs, A. Kreyssig, K. Nenkov, S. Shulga, K.-H. Muller, and L. Schultz, Physica C **306**, 1 (1998).
[50] Due to the nonspherical, multiband character of the Fermi surface, the approximation of α based on the relation $\sqrt{2}H^*_{c2}(0\,\mathrm{K})/18.4T_{c0}$ gives 0.4 which is an unreasonably high value.
[51] M. Xu, P. C. Canfield, J. E. Ostenso, D. K. Finnemore, B. K. Cho, Z. Wang, and D. C. Johnston, Physica C **227**, 321 (1994).
[52] H. Bitterlich, W. Loser, K. Nenkov, G. Fuchs, K. Winzer, and L. Shultz, Physica C **284–288**, 487 (2000).
[53] H. Bitterlich, W. Loser, G. Behr, K. Nenkov, G. Fuchs, A. Gumbel, and L. Shultz, Physica C **321**, 93 (1999).
[54] B. K. Cho, H. B. Kim, and S.-I. Lee, Phys. Rev. B **63**, 144528 (2001).